

Clathrin-dependent endocytosis is required for immunity mediated by pattern recognition receptor kinases

Malick Mbengue [a], Gildas Bourdais [a], Fabio Gervasi [a], [b], Martina Beck [a], Ji Zhou (周济) [a], Thomas Spallek [a], Sebastian Bartels [c], Thomas Boller [c], Takashi Ueda [d], Hannah Kuhn [a], [e], and Silke Robatzek [a]

[a] The Sainsbury Laboratory, Norwich NR4 7UH, United Kingdom;

[b] Fruit Tree Research Center, Council for Agricultural Research and Economics, 00134 Rome, Italy; [c] Zürich-Basel Plant Science Center, Department of Environmental Sciences, Botany, University of Basel, CH-4056 Basel, Switzerland;

[d] National Institute for Basic Biology, Aichi 444-8585, Japan; and

[e] Unit of Plant Molecular Cell Biology, Institute for Biology I, RWTH Aachen University, 52056 Aachen, Germany

Abstract: Sensing of potential pathogenic bacteria is of critical importance for immunity. In plants, this involves plasma membrane-resident pattern recognition receptors, one of which is the FLAGELLIN SENSING 2 (FLS2) receptor kinase. Ligand-activated FLS2 receptors are internalized into endosomes. However, the extent to which these spatiotemporal dynamics are generally present among pattern recognition receptors (PRRs) and their regulation remain elusive. Using live-cell imaging, we show that at least three other receptor kinases associated with plant immunity, PEP RECEPTOR 1/2 (PEPR1/2) and EF-TU RECEPTOR (EFR), internalize in a ligand-specific manner. In all cases, endocytosis requires the coreceptor BRI1-ASSOCIATED KINASE 1 (BAK1), and thus depends on receptor activation status. We also show the internalization of liganded FLS2, suggesting the transport of signaling competent receptors. Trafficking of activated PRRs requires clathrin and converges onto the same endosomal vesicles that are also shared with the hormone receptor BRASSINOSTEROID INSENSITIVE 1 (BRI1). Importantly, clathrin-dependent endocytosis participates in plant defense against bacterial infection involving FLS2-mediated stomatal closure and callose deposition, but is uncoupled from activation of the flagellin-induced oxidative burst and MAP kinase signaling. In conclusion, immunity mediated by pattern recognition receptors depends on clathrin, a critical component for the endocytosis of signaling competent receptors into a common endosomal pathway.

Significance: Plants detect conserved molecular patterns of pathogens via cell surface-localized receptors, such as the flagellin receptor kinase FLS2, that initiate effective plant immunity. Activated FLS2 is endocytosed, but the degree to which other receptor kinases exhibit similar spatiotemporal dynamics remains unclear. We show that internalization into a common endosomal pathway after ligand perception is a general phenomenon of the tested receptor kinases, including the danger peptide receptor PEPR1. FLS2 endocytosis is mediated by clathrin and is uncoupled from the regulation of acute pathogen-induced responses, but is involved in steady defenses and contributes to plant immunity against bacterial infection. We propose that clathrin-dependent internalization of ligand-activated receptor kinases into a common endosomal pathway facilitates the responses required for full plant immunity.

Keywords: *pattern-triggered immunity; clathrin; FLS2; PEPR1; EFR*

The plasma membrane forms the primary interface of eukaryotic cells to sense potentially invading pathogens. The recognition of microbe-associated molecular patterns (MAMPs) at the plasma membrane is mediated by pattern recognition receptors (PRRs), critical components of the plant's innate immune system. A wide range of distinct PRRs for conserved microbial patterns have been characterized, including more than 10 PRRs with known ligands in *Arabidopsis thaliana* (1, 2). A well-studied PRR is FLAGELLIN SENSING 2 (FLS2), a receptor kinase recognizing a conserved peptide domain of the bacterial flagellin (flg22) and conferring antibacterial immunity (2). Upon flg22 binding, FLS2 forms a signalling competent complex with the receptor kinase BRI1-ASSOCIATED KINASE 1/SOMATIC EMBRYOGENESIS RECEPTOR KINASE 3 (BAK1/SERK3) (3, 4). This activation initiates downstream immune responses and the internalization of FLS2 from the plasma membrane into endosomes (5).

BAK1 is a coreceptor shared with many plasma membrane-located receptors. In addition to FLS2, these include the PRR kinases EF-TU RECEPTOR (EFR) recognizing bacterial EF-TU through its elicitor-active epitope elf18 (1), receptors for damage-associated endogenous peptides such as PEP RECEPTOR 1 (PEPR1) and PEPR2 that perceive peptides of the AtPep family (6), and the brassinosteroid (BL) hormone receptor BRASSINOSTEROID INSENSITIVE 1 (BRI1) (7). Therefore, it is important to establish whether these distinct BAK1-dependent receptors are internalized from the plasma membrane through similar endocytic routes, and also how endocytosis relates to immunity.

In contrast to the constitutive endocytosis of BRI1 (7–9), FLS2 internalization is triggered upon flg22 perception (5). This induces trafficking of FLS2 into the late endosomal pathway and is associated with receptor degradation (10, 11). Induced trafficking into late endosomes was also observed for the receptor-like proteins Cf-4 and LeEix2, which recognize fungal Avr4 and xylanase, respectively (12, 13). While this depended on BAK1/SERK3 for Avr4-induced Cf-4 internalization (12), BAK1 was not required for xylanase-triggered endocytosis of LeEix2 (13). Thus, although internalization of PRRs (FLS2, LeEix2, and Cf-4) is found in plants, whether receptor-mediated endocytosis is a more general feature of activated PRRs and involves shared trafficking routes remains unclear.

Here we used live cell confocal imaging aided by quantitative computational image analysis to demonstrate that all tested PRRs undertake receptor-mediated endocytosis following ligand perception through a common endosomal route and to determine the role of clathrin in this process.

Results and Discussion

Ligand-Induced Internalization Is Conserved Across PRR Families. In this study, we addressed whether ligand-induced endocytosis is more widely present among the receptors of the immune system, and focused on PEPR1/2 and EFR, PRRs of the receptor kinase family with high ligand binding affinities and specificity for a single ligand. To establish whether PEPR1 and PEPR2 receptor kinases are internalized upon stimulation with pep1, we investigated stable *Arabidopsis* lines that express the C-terminally YFP-tagged receptors. Ligand-induced internalization of PEPR1-YFP and PEPR2-YFP was detected in *Arabidopsis* leaves (Fig. 1A), and a time course analysis revealed kinetics of PEPR1-YFP internalization comparable to those of FLS2-GFP endocytosis (Fig. 1B) (5). Importantly, we observed ligand-induced internalization of PEPR1 and FLS2 after heterologous expression in *Nicotiana benthamiana* leaves (Fig. 1C), a suitable model plant for studying MAMP-triggered immune responses (14). In both *Arabidopsis* and *N. benthamiana*, PEPR1-YFP fusion proteins were present at the plasma membrane and relocalized into vesicles upon pep1 elicitation (Fig. 1 A and C). As reported previously (15), *N. benthamiana*-expressed FLS2-GFP localized to the plasma membrane and was internalized when triggered with flg22 or wild type (WT) *Pseudomonas syringae* pv. tomato

DC3000 (Pto DC3000) extracts (Fig. 1 C and D). Flg22-induced internalization was also observed for homologous expression of NbFLS2 (Fig. S1). Taken together, these findings suggest conservation of PRR trafficking between species.

The study of *N. benthamiana* also allows us to visualize EFRGFP, which cannot be detected in microscopy images of EFR-GFP transgenic *Arabidopsis* plants despite functional complementation (16). We observed plasma membrane localization of EFR-GFP after heterologous expression in *N. benthamiana* leaves, and EFRGFP relocated into vesicles upon elf18 elicitation (Fig. 1C). In each instance, ligand treatment not matching the cognate PRR, or the use of a Pto DC3000 extract devoid of flagellin, did not result in receptor relocation from the plasma membrane (Fig. 1 C and D). Thus, ligand-specific internalization is present among several PRRs with similar dynamics to FLS2.

Signaling-Competent PRRs Are Internalized. We next addressed whether ligand-induced endocytosis of PRRs in *N. benthamiana* also depends on the receptor activation status and function of the coreceptor BAK1/SERK3 as found for FLS2 in *Arabidopsis* (5). Using virus-induced gene silencing, we knocked down NbSERK3a/b, two closely homologous genes to *Arabidopsis* BAK1 (17), and analyzed the subcellular localization of transiently expressed PEPR1, FLS2, and EFR fusion proteins. In contrast to controls, NbSERK3a/b-silenced leaves were inhibited for induced internalization of PEPR1, FLS2, and EFR (Fig. S2A). Thus, and despite *N. benthamiana* lacking PEPR1 or EFR homologs, ligand-induced endocytosis of these transiently expressed receptors was dependent on the same coreceptor, indicating strong similarities with the FLS2 and Cf-4 trafficking pathways.

Flg22 induces and stabilizes FLS2-BAK1 complexes to promote receptor signaling (3, 4). Thus, receptor-mediated endocytosis could result in the concomitant uptake of the ligand with the receptor, raising the possibility that signaling-competent receptors are transported. To investigate this possibility, we treated *Arabidopsis* cotyledons with TAMRA-flg22, an N-terminally labeled fluorescent flg22 (18). TAMRA-flg22 is comparably biologically active to flg22 when measured as inhibition of *Arabidopsis* seedling growth (Fig. S2B).

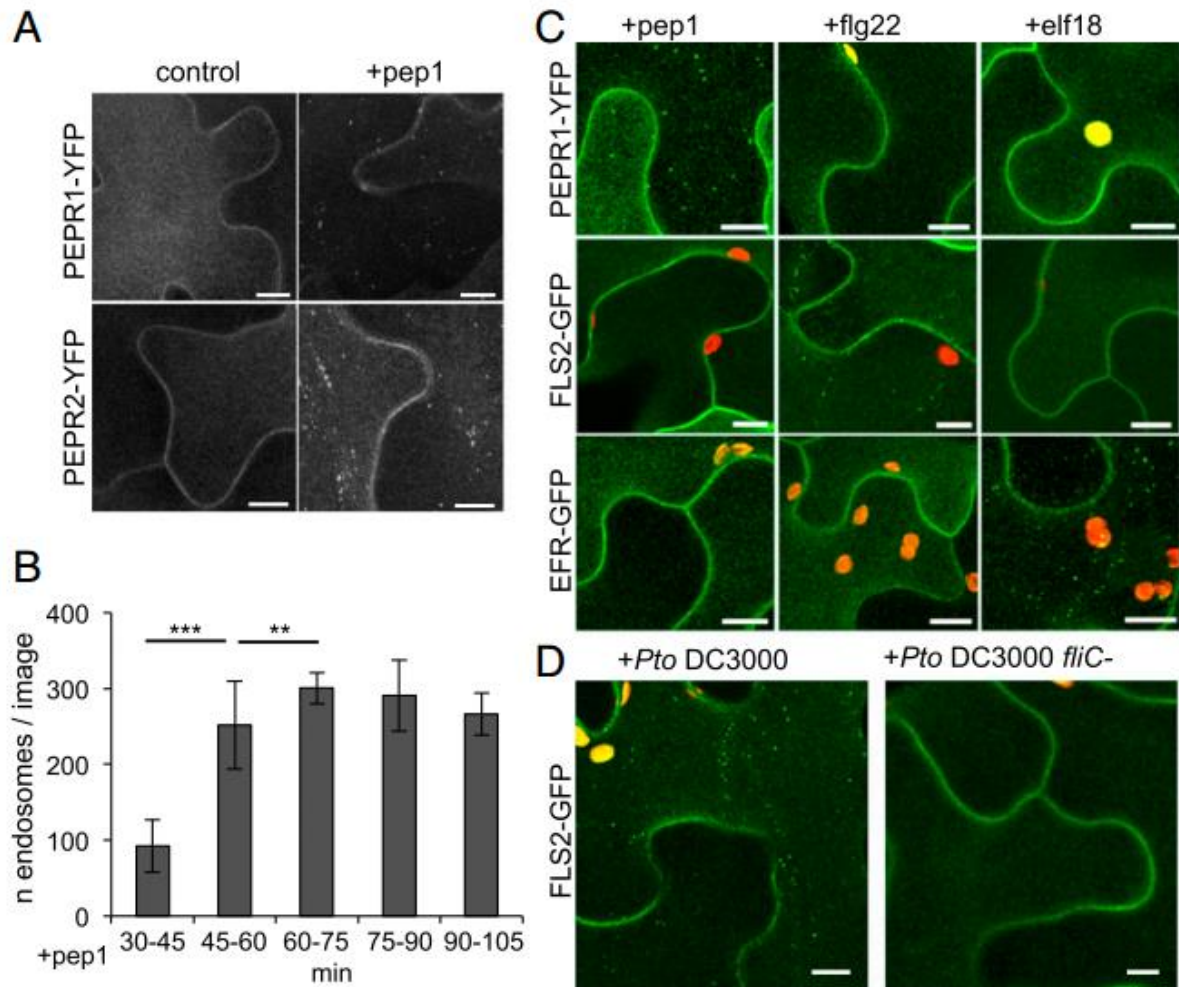


Fig. 1. Ligand-induced endocytosis is conserved across PRRs. (A) Cotyledons of *A. thaliana* seedlings stably expressing PEPR1-YFP and PEPR2-YFP, as indicated, were treated with water or with pep1 for 40 min before imaging. Arrows point to PEPR1-YFP and PEPR2-YFP endosomes. Micrographs are maximum projections of 21 optical sections every 1 μm of z-distance. (Scale bars: 10 μm .) (B) Bar graphs representing the average \pm SD number of PEPR1-YFP endosomes detected per 15-min time interval in *A. thaliana* cotyledons treated with pep1. (C and D) Confocal micrographs of *N. benthamiana* leaf epidermal cells expressing PEPR1-YFP, FLS2-GFP, and EFR-GFP challenged with pep1, flg22, and elf18 elicitor peptides, or total extracts of *Pto* DC3000 strains, as indicated. All constructs were expressed in *N. benthamiana* leaves, and treatments were performed 80 min before imaging. Micrographs are maximum projections of 8–12 confocal optical sections taken using a 1- μm z-distance. Chloroplast autofluorescence was recorded simultaneously in the red channel. (Scale bars: 10 μm .)

In epidermal leaf cells of the FLS2-GFP complemented *fls2* null mutant, TAMRA-flg22 was observed in mobile vesicles, and FLS2-GFP colocalized with these vesicles (Fig. 2). No vesicles were observed in TAMRA-flg22-treated *fls2* and *bak1-3* mutant plants (Fig. 2 and Fig. S2C), in agreement with FLS2-GFP internalization requiring BAK1 function (5). Taken together, these findings demonstrate the receptor-dependent uptake of the peptide into FLS2-GFP-positive endosomes that might explain the irreversible flg22 binding when using intact cells, but not when using plant extracts (19). This finding is an example of receptor-mediated cointernalization of ligands in plants, reminiscent of a brassinosteroid fluorescent analog colocalizing with BRI1 (9), and demonstrates the internalization of liganded, signaling-competent FLS2 receptors. Liganded FLS2 is destined to the vacuole, as evidenced by TAMRA-flg22 accumulation (Fig. S2D).

The heterodimerization of FLS2 with BAK1 is driven by their extracellular domains and is independent of their kinase activities (3, 20).

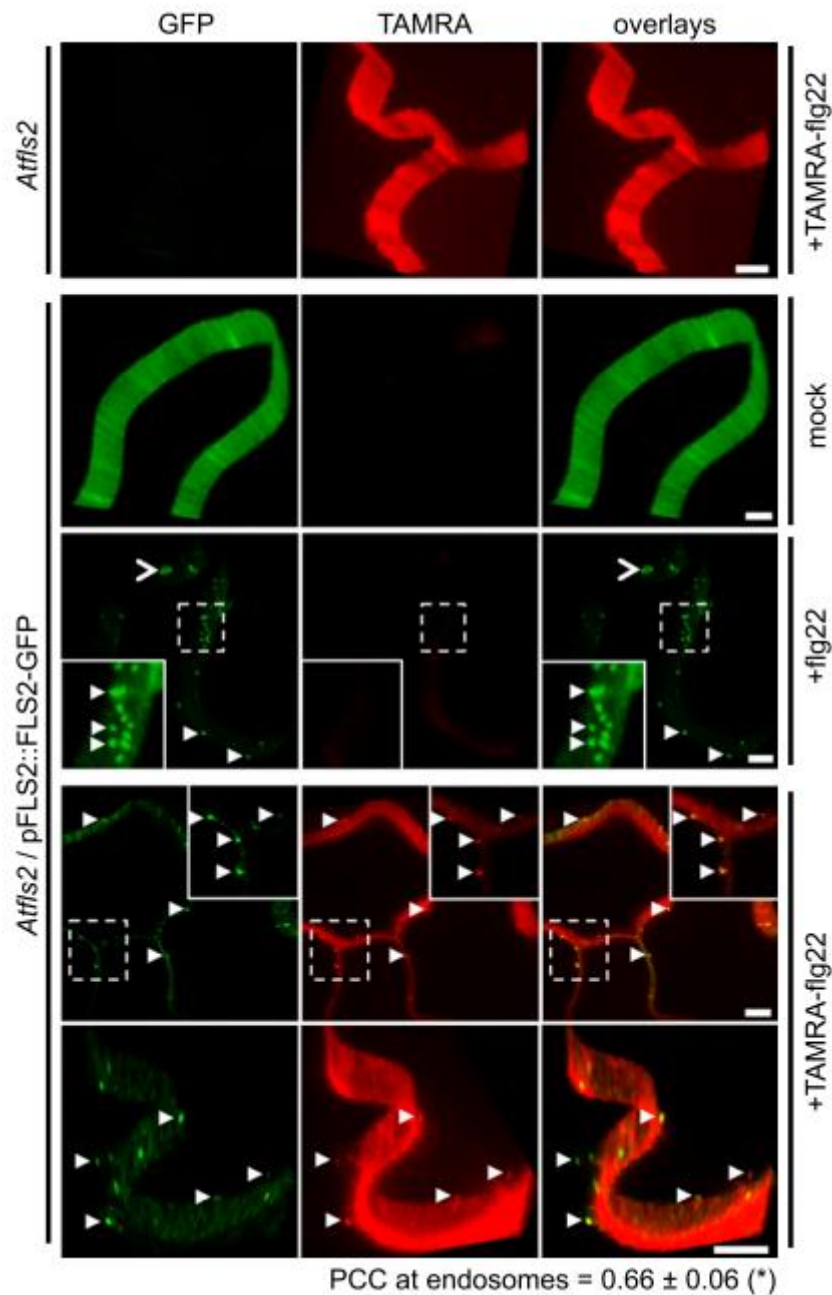


Fig. 2. Flg22 is internalized together with FLS2. Representation of a z-projected 2-min time series of epidermal cells of the indicated genotypes after incubation with 10 μ M TAMRA-flg22 for 80 min (fls2 for 120 min). Insets (dashed lines) are magnified in the bottom panel. White arrowheads point to endosomes, and open arrowheads point to chloroplasts. (Left) Fluorescence signals recorded in the green (FLS2-GFP) channels. (Middle) Fluorescence signals recorded in the red (TAMRA-flg22) channels. (Right) Fluorescence signals recorded in the overlaid channels. (Scale bars: 5 μ m.) PCC, Pearson's correlation coefficient. $n = 3$. * $P (n - 2) < 0.01$.

To test whether FLS2 internalization after flg22 perception requires its kinase activity, we monitored the subcellular behaviour of the kinase-inactive variant FLS2D997N (20). Expression of FLS2D997N-GFP was detected only at the plasma membrane irrespective of flg22 treatment (Fig. S2E). Taken

together, these results indicate that endocytosis of FLS2 requires reconstitution of an active signaling receptor complex that goes beyond recruitment of SERK3s.

Activated PRRs Share a Similar Trafficking Pathway. The observation that activated PRRs are internalized in a ligand-specific manner prompted us to investigate whether the different receptors would be present at distinct endosomal vesicles. To do so, we treated cotyledons of PEPR1-YFP Arabidopsis lines with pep1 in combination with TAMRA or TAMRA-flg22. PEPR1-YFP was observed in vesicles, and TAMRA-flg22, but not TAMRA alone, colocalized to these vesicles (Fig. 3A). To corroborate and extend these findings, we performed colocalization studies after pairwise heterologous expression of PEPR1, FLS2, and EFR in *N. benthamiana* leaves. Coexpression of differentially labeled FLS2-GFP and FLS2-mCherry showed a strong colocalization at endosomes when elicited with flg22 (Fig. S3A). We then coexpressed PEPR1-YFP or EFR-GFP with FLS2-mCherry. Flg22 treatment specifically induced endocytosis of FLS2-mCherry, but not of PEPR1-YFP (Fig. 3B), further illustrating that the endocytosis of these receptors is highly ligand-specific. Pep1 and flg22 coelicitation induced endocytosis of PEPR1-YFP and FLS2-mCherry, which exhibited colocalization at endosomes (Fig. 3B). Likewise, elicitation with elf18 specifically triggered EFR-GFP endocytosis, whereas FLS2-mCherry maintained its plasma membrane localization (Fig. 3C). Cotreatments with elf18 and flg22 induced endocytosis of both EFR-GFP and FLS2-mCherry, and they colocalized at endosomes (Fig. 3C). PEPR1-YFP and EFR-GFP colocalized at FLS2-mCherry endosomes with a similar Pearson's correlation coefficient value as for the FLS2-GFP/FLS2-mCherry pair (Fig. 3D). These observations suggest that activated PRRs share trafficking into a common endosomal pathway.

To support our findings, we tested whether PEPR1 and EFR traffic along the same endocytic pathway as revealed for FLS2 (5, 15), and pairwise coexpressed in *N. benthamiana* leaves PEPR1-YFP, FLS2-GFP, and EFR-GFP with markers of the Golgi apparatus (MEMB12), the trans-Golgi network (TGN; Vha-A1), and two partially overlapping populations of endosomes (ARA7/RabF2b and ARA6/RabF1). Upon cognate ligand elicitation, vesicles positive for each receptor showed colocalization with mCherry-ARA7/RabF2b-labelled and ARA6/RabF1-RFP-labelled endosomes, whereas no colocalization was observed with MEMB12-mCherry or Vha-A1-RFP (Fig. S4A). This was further supported by the Pearson's correlation coefficient values calculated at endosomes (Fig. S4B). There was no evidence of involvement of the autophagy machinery in FLS2 endocytosis (Fig. S5 A–C). These observations reveal that like FLS2, activated PEPR1 and EFR are cargoes of the late endocytic trafficking route. Interestingly, the internalization-deficient FLS2D997N-GFP colocalized with FLS2-mCherry at endosomes after flg22 treatment (Fig. S3B). Because FLS2 can form homo-oligomers in the absence and presence of flg22 (21), we hypothesize that FLS2D997N is internalized as oligomer complex together with signaling-competent FLS2 (4).

Endosomal Trafficking of Activated PRRs Is Shared with BRI1. Endocytosis is also known for the BAK1-dependent hormone receptor BRI1 (8, 9). To gain insight into BRI1 trafficking in *N. benthamiana* leaves, we pairwise-coexpressed BRI1-GFP with MEMB12-mCherry, Vha-A1-RFP, mCherry-ARA7/RabF2b, and ARA6/RabF1-RFP. BRI1-positive vesicles colocalized with the endosomal markers ARA7/RabF2b and ARA6/RabF1-RFP (Fig. S6A), in agreement with BRI1 vacuolar trafficking (22). Heterologous coexpression of BRI1-GFP and FLS2-mCherry in *N. benthamiana* revealed colocalization at vesicles after flg22 elicitation (Fig. S6B). Colocalization of BRI1-GFP at FLS2-mCherry endosomes occurred with a similar Pearson's correlation coefficient value as for the FLS2-GFP/FLS2-mCherry pair. Like heterologously expressed BRI1-GFP in *N. benthamiana*, cotyledons of stably expressing BRI1-GFP Arabidopsis lines showed the presence of BRI1 at the plasma membrane and mobile vesicles. TAMRA-flg22 colocalized to these vesicles (Fig. S6C).

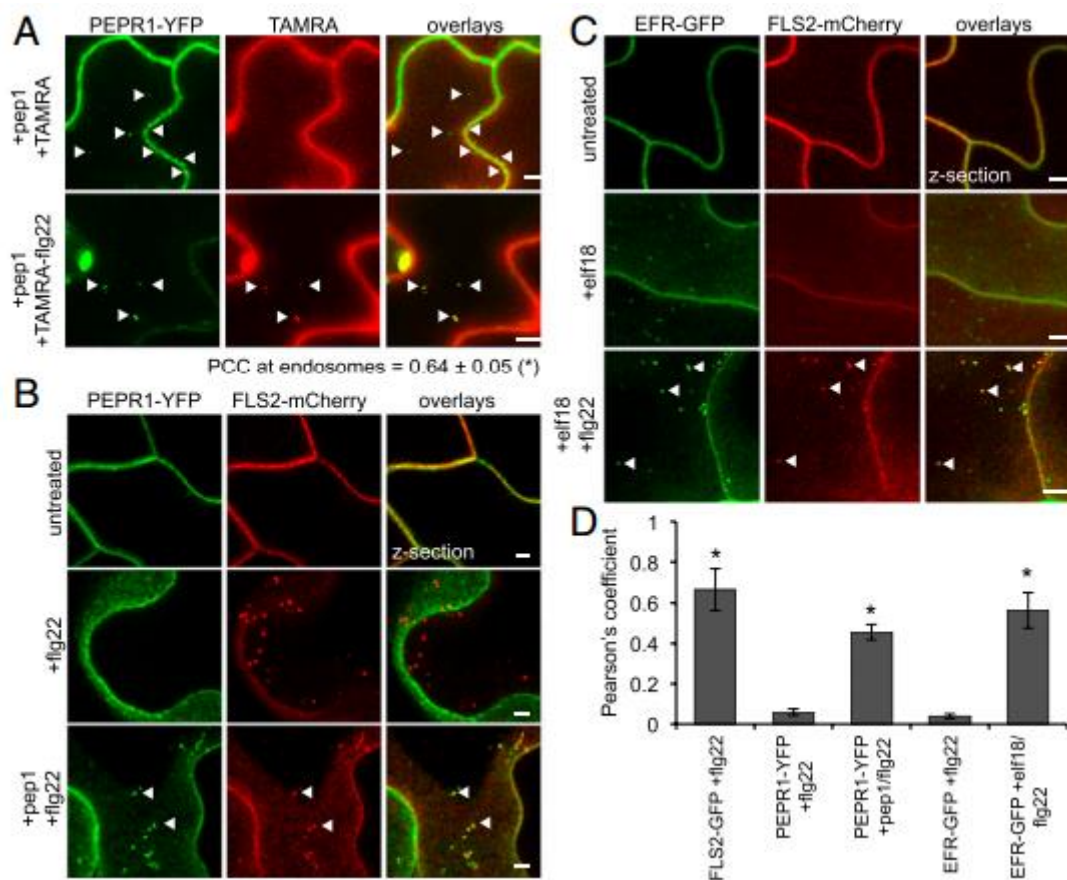


Fig. 3. Ligand-activated PRRs colocalize at endosomes. (A) PEPR1-YFP localization at 45 min after a 10-s cotreatment with pep1 and TAMRA or with pep1 and TAMRA-flg22. Arrowheads point to endosomal signals of either PEPR1-YFP or TAMRA-flg22. (Scale bars: 5 μ m.) Micrographs are maximum projections of 10–12 confocal optical sections taken using a 0.5- μ m z-distance. $n = 6$. * $P(n - 2) < 0.05$. (B) PEPR1-YFP and FLS2-mCherry localization before and after simultaneous flg22 and pep1/flg22 treatments. (C) EFR-GFP and FLS2-mCherry localization before and after simultaneous elf18 and elf18/flg22 treatments. In B and C, all constructs are expressed in *N. benthamiana* leaves. Micrographs are maximum projections of 8–12 confocal optical sections taken using a 1- μ m z-distance unless indicated otherwise. (Left) Green channels. (Middle) Red channels. (Right) Overlaid channels. White arrowheads point to colocalized signals at endosomes. Peptide treatments were performed 80 min before imaging. (Scale bars: 5 μ m.) (D) Bar graphs showing the average \pm SD Pearson's correlation coefficient at endosomes between FLS2-mCherry and the coexpressed receptor after elicitor treatments, as indicated. $n = 3$. * $P(n - 2) < 0.01$.

Internalization of Activated PRRs Depends on Clathrin. Both clathrin-independent and -dependent internalization mechanisms have been described in plants (23, 24). Because clathrin has been shown to function in BRI1 endocytosis (9), we addressed genetically whether clathrin is required for the internalization of PRRs. To overcome potential genetic redundancy, we knocked down the six CLATHRIN HEAVY CHAIN (NbCHC) constructs found in the *N. benthamiana* genome (25) by transient expression of a single hairpin construct (Fig. S7A). Heterologously expressed FLS2-GFP exhibited normal plasma membrane localization in NbCHC-silenced *N. benthamiana* leaves. Quantification of FLS2 endosomes after flg22 treatment revealed an approximate 75% decrease in NbCHC-silenced leaves vs. control (Fig. 4A and Fig. S7B). Pep1-induced endosomal numbers of PEPR1-YFP were reduced by approximately 50% in NbCHC-silenced leaves (Fig. S7C). In the case of FLS2, we observed an increase in average size for the remaining endosomes detected in NbCHC-silenced leaves (Fig. 4A), which can be explained by a concomitant decrease in the numbers of small

endosomes and the presence of abnormally enlarged structures. These structures did not colocalize with mCherry-ARA7/RabF2b, indicating defects in the normal endosomal trafficking of FLS2- GFP (Fig. S7D). We also noticed that the mCherry-ARA7/ RabF2b-positive vesicles were increased in size (Fig. S7D), consistent with the involvement of clathrin in vesicle trafficking from the TGN/early endosome (26). These data suggest that clathrin plays a role in the endocytosis of FLS2 and PEPR1 receptors. In Arabidopsis, two related genes, CHC1 and CHC2, encode clathrin heavy chains, of which chc2 mutants were shown to affect endocytic events from the plasma membrane (23). To investigate whether FLS2 endocytosis is mediated by CHC2 in Arabidopsis, we treated cotyledons of chc2-1 mutants with TAMRA-flg22. Microscopic observation and quantification revealed that TAMRA-flg22-positive vesicles increased in WT cotyledons to a maximum level at 40–60 min after treatment (Fig. 4B and Fig. S8A), mirroring the dynamic behavior of ligand-induced FLS2 endocytosis (5). In contrast, the number of TAMRA-flg22-positive vesicles remained unchanged above background noise in chc2-1 cotyledons (Fig. 4B). Similar results were obtained with the independent chc2-3 mutant allele (Fig. S9A).

Clathrin Is Required for Immunity Against Bacterial Infection. Our cell biology studies revealed that endocytosis of plasma membranelocated receptors triggering plant immunity is dependent on clathrin function. This finding provided an opportunity to address whether PRR-mediated immunity is associated with trafficking by clathrin. Thus, we examined the growth of Pto DC3000 and two virulencecompromised strains in chc2-1 mutant lines. Following spray infection of fully virulent Pto DC3000, a strain lacking coronatine (cor-) known to promote bacterial entry through stomata (27), and a strain defective in type III secretion of virulence effectors (hrcC-), growth of all bacterial strains was significantly higher in chc2-1 mutants compared with Col-0 WT (Fig. 4C). Similar results were obtained in chc2-3 mutants (Fig. S9B), and are consistent with increased Pto DC3000 and Pto DC3000 hrcC- infection in knockout mutants of DYNAMIN-RELATED PROTEIN (DRP) 2b (28), components associated with the clathrin machinery. Bacteria grew to similar levels in chc1-1 and chc1-2 mutants compared with Col-0 WT (Fig. S10 A and B). This finding confirms a specific role of CHC2 as a positive regulator of defense against bacteria independent of the delivery of cor- and type III secreted effectors.

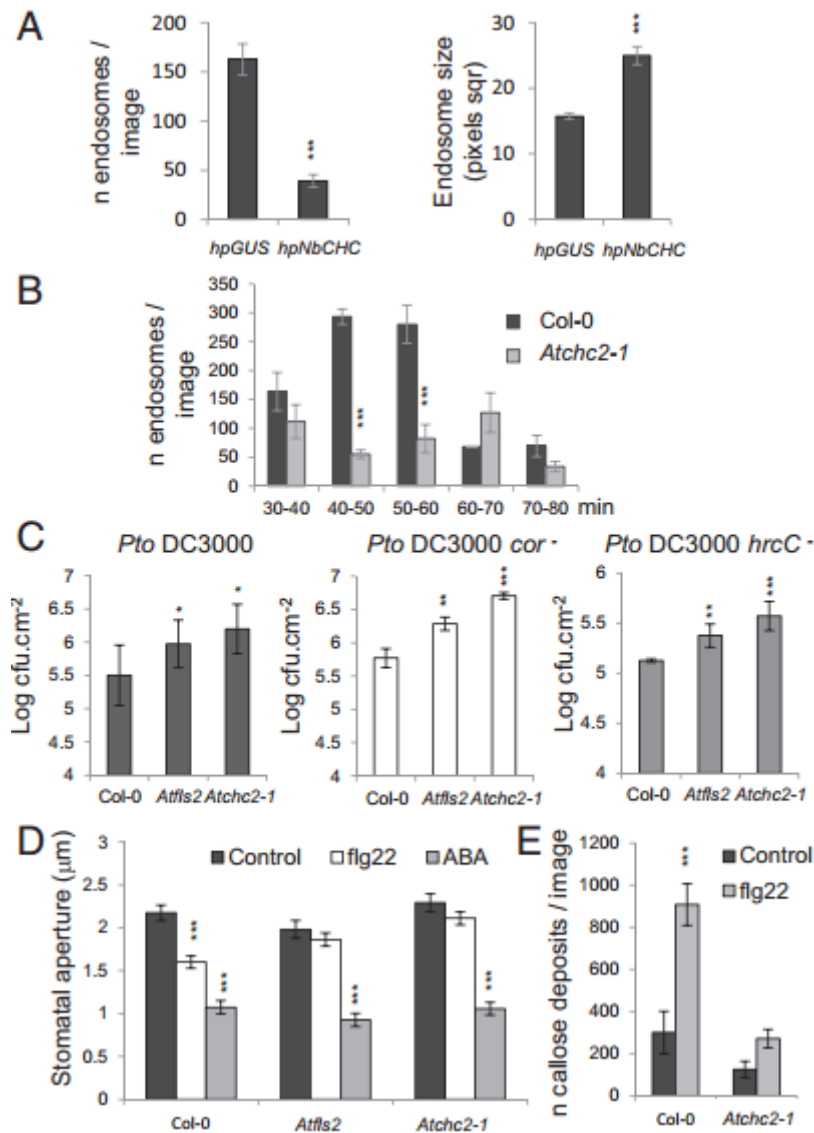


Fig. 4. Clathrin regulates FLS2 internalization and flg22-induced immune responses. (A) Bar graphs showing the average \pm SE number and size of FLS2- GFP endosomes detected per image in control and clathrin-silenced leaves (untreated, $n = 7$ images; flg22 treated, $n = 25$ images pooled from two biological replicates). (B) Bar graph showing the average \pm SE number of TAMRA-flg22 endosomes detected per 10-min time interval in *A. thaliana* Col-0 and *chc2-1* cotyledons treated with TAMRA-flg22. (C) Plants of the indicated genotypes were surface-inoculated with *Pto* DC3000, *Pto* DC3000 *cor*⁻, and *Pto* DC3000 *hrcC*⁻, and bacterial growth was examined at 3 dpi. Bars represent mean \pm SE values. $n = 8$. Experiments were repeated independently at least twice, with similar results. (D) Quantification of aniline blue-stained callose deposits per image of the indicated genotypes and treatments. Bars represent mean \pm SD. $n = 19$ from two independent experiments. (E) Stomatal apertures of the indicated genotypes were measured following the indicated treatments. Bars represent the average \pm SE aperture from two independent experiments; average $n = 92$. * $P < 0.05$; ** $P < 0.01$; *** $P < 0.001$, Student's *t* test.

Clathrin Is Not Required for PRR-Mediated Acute Immune Responses. PRR-mediated immunity involves the activation of various defense responses, including the generation of reactive oxygen species (ROS), activation of MAP kinases, stomatal closure, and callose deposition (2). We tested whether the inhibition of clathrin-mediated endocytosis interferes with any of these MAMP responses. The flg22-induced ROS production mediated by the plasma membrane NADPH oxidase RbohD in *Arabidopsis* was little affected in leaves of *chc2-1* mutants, which exhibited slightly elevated ROS during its down-regulation compared with Col-0 WT (Fig. S8 B and C); however, we did

not observe vastly prolonged production of ROS, indicating that down-regulation of the flg22-induced ROS burst is independent of FLS2 endocytosis. Similar results were obtained in NbCHC-silenced *N. benthamiana* leaves (Fig. S7E). These findings demonstrate that the ROS burst is most likely conferred by plasma membrane-localized FLS2, in line with the activation of RbohD via an upstream calcium influx, calcium-dependent protein kinases, and BOTRYTIS INDUCED KINASE (BIK1) (29, 30). Although our results are in disagreement with other findings showing opposing outcomes of either strongly reduced or prolonged oxidative bursts upon inhibition of flg22-induced FLS2 degradation or endocytosis, respectively (31, 32), we cannot exclude the possibility of additional effects from the chemical approaches used in these studies or from the activities of clathrin-mediated endocytosis regulating RbohD localization (33). Knockout of CHC1 did not alter the flg22-triggered ROS burst (Fig. S10C). We next monitored the activation of MAPKs found to be phosphorylated on MAMP treatment in *Arabidopsis* (2). Activation of MAPKs was induced at 15 and 30 min after flg22 elicitation in WT and *chc2-1* plants (Fig. S8D). In both Col-0 WT and *chc2-1*, MAPK activation returned to basal levels by 60 min after treatment. Similarly, flg22 treatment induced activation of MAPK in NbCHC-silenced *N. benthamiana* leaves (Fig. S7F). These results suggest that clathrin is not required for the transient activation of MAPKs, and are consistent with previous results obtained from chemical interference and *drp2b* mutants (11, 28). Although it is possible that both clathrin depletion in *N. benthamiana* leaves and *chc2* knockout in *Arabidopsis* do not fully inhibit endocytosis, our data suggest that plasma membrane-resident FLS2 is sufficient to induce transient MAPK activation.

Clathrin Is Involved in PRR-Mediated Callose Deposition and Stomatal Closure. An important component of MAMP-mediated immunity is the restriction of pathogen entry through closure of stomata (27). To invade leaves, *Pto* DC3000 secretes *cor-*, which triggers stomatal opening. Therefore, we measured stomatal apertures under control conditions and after treatment with flg22 and abscisic acid (ABA), a hormone that induces stomatal closure in drought stress. We found that stomatal closure induced by flg22, but not by ABA, was significantly impaired in *chc2-1* mutants (Fig. 4D). Flg22 elicited the closure of stomata in *chc1* loss-of-function mutants (Fig. S10D). These results indicate that CHC2, but not CHC1, participates in flg22-triggered stomatal immunity, thereby leading to the increased growth of *Pto* DC3000 *cor-* bacteria in *chc2*, but not *chc1*, mutants. Thus, endocytosis of FLS2 appears to be positively correlated with stomatal immunity, consistent with impaired flg22-induced stomatal closure and FLS2 endosomal sorting in *vps37-1* mutants (10). Given that the flg22-induced ROS burst, a critical response in stomatal closure (30), was not impaired in *chc2* mutants, we also quantified the deposition of callose, which has been implicated in stomatal closure (34), in response to flg22. We found that Flg22-induced callose deposition was significantly impaired in *chc2-1* and *chc2-3* mutants compared with Col-0 WT (Fig. 4E and Fig. S9C). No difference in callose deposition was observed between wounded *chc2-1* and Col-0 WT (Fig. S8E), demonstrating that CHC2 is specifically required for flg22-induced callose deposition. Interestingly, *chc2* mutants exhibited enhanced callose deposition on infection with the *Erysiphe cichoracearum* fungal pathogen (35), which could involve aspects of effector-triggered immunity. The finding that flg22-induced callose deposition is inhibited in *chc2* mutants contrasts with the WT-like and increased callose deposition in flg22-treated *vps37-1* and *drp2b* mutants, respectively (10, 28); however, both *vps37-1* and *drp2b* exhibited mildly reduced FLS2 endocytosis. It is also possible that clathrin or DRP2b affects the plasma membrane localization of POWDERY MILDEW RESISTANT4 (PMR4), the callose synthase responsible for flg22-induced callose production (2).

Our data reveal that ligand-induced endocytosis is a conserved mechanism integral to the cellular dynamics of all tested PRR kinases of the plant's immune system. The finding that distinct activated

receptors colocalize at endosomes reveals converging endocytic routes that likely join at ARA7/RabF2b endosomes. This highlights a common pathway for the transport of activated plant receptors, supporting the hypothesis that all receptors are targeted to the same final destination, possibly the vacuole. This extends to the receptor-like protein PRRs Cf-4 and LeEix2, which reportedly localize to late endosomes (12, 13), as well as to the BRI1 hormone receptor. It provides evidence that this pathway is common across different types of PRR families and receptor kinases, possibly to accumulate cargoes before delivery to the vacuole. Interestingly, pathogens secrete effectors that interfere with DRP2 function and cause the relocation of endosomal FLS2 to infection sites (36, 37) indicating that this common endosomal pathway is targeted by pathogens to suppress PRR-mediated immunity. Our receptor coexpression and ligand uptake experiments revealed that only liganded PRRs were internalized, demonstrating the specificity of receptor-mediated endocytosis. This implies the absence of strong molecular interactions between these distinct receptors, although all engage with BAK1 to reconstitute active signaling complexes required for their endocytosis. Using clathrin knockout to genetically inhibit PRR internalization, we determined that acute flg22-triggered responses are most likely conferred from the plasma membrane. Nevertheless, we found that CHC2 is a positive regulator of flg22-induced callose deposition and stomatal immunity contributing to the defenses against bacterial infection (10, 28). Thus, our observations provide evidence that CHC2-mediated endocytosis positively affects MAMP-triggered immunity, and establish that the regulation of endocytic trafficking is critical for the full deployment of plants' immune response to pathogen attack.

Acknowledgements: We thank members of the S.R. laboratory for fruitful discussions, H. Häweker for technical support, and C. Zipfel and S. Kamoun for reading the manuscript. We thank S. Somerville (Stanford University), N. Patron (Norwich University), and C. Zipfel (Norwich University) for providing materials. M.B. was supported by a fellowship from the German Research Foundation, G.B. and S.R. are supported by a grant from the European Research Council, and S.R. is supported by the Gatsby Charitable Foundation.

References:

1. Böhm H, Albert I, Fan L, Reinhard A, Nürnberger T (2014) Immune receptor complexes at the plant cell surface. *Curr Opin Plant Biol* 20:47–54.
2. Boller T, Felix G (2009) A renaissance of elicitors: Perception of microbe-associated molecular patterns and danger signals by pattern-recognition receptors. *Annu Rev Plant Biol* 60:379–406.
3. Sun Y, et al. (2013) Structural basis for flg22-induced activation of the Arabidopsis FLS2-BAK1 immune complex. *Science* 342(6158):624–628.
4. Somssich M, et al. (2015) Real-time dynamics of peptide ligand-dependent receptor complex formation in planta. *Sci Signal* 8(388):ra76.
5. Beck M, Zhou J, Faulkner C, MacLean D, Robatzek S (2012) Spatio-temporal cellular dynamics of the Arabidopsis flagellin receptor reveal activation status-dependent endosomal sorting. *Plant Cell* 24(10):4205–4219.
6. Tang J, et al. (2015) Structural basis for recognition of an endogenous peptide by the plant receptor kinase PEPR1. *Cell Res* 25(1):110–120.
7. Russinova E, et al. (2004) Heterodimerization and endocytosis of Arabidopsis brassinosteroid receptors BRI1 and AtSERK3 (BAK1). *Plant Cell* 16(12):3216–3229.
8. Geldner N, Hyman DL, Wang X, Schumacher K, Chory J (2007) Endosomal signaling of plant steroid receptor kinase BRI1. *Genes Dev* 21(13):1598–1602.

9. Irani NG, et al. (2012) Fluorescent castasterone reveals BRI1 signaling from the plasma membrane. *Nat Chem Biol* 8(6):583–589.
10. Spallek T, et al. (2013) ESCRT-I mediates FLS2 endosomal sorting and plant immunity. *PLoS Genet* 9(12):e1004035.
11. Smith JM, Salamango DJ, Leslie ME, Collins CA, Heese A (2014) Sensitivity to Flg22 is modulated by ligand-induced degradation and de novo synthesis of the endogenous flagellin-receptor FLAGELLIN-SENSING2. *Plant Physiol* 164(1):440–454.
12. Postma J, et al. (2016) Avr4 promotes Cf-4 receptor-like protein association with the BAK1/SERK3 receptor-like kinase to initiate receptor endocytosis and plant immunity. *New Phytol* 210(2):627–642.
13. Bar M, Sharfman M, Ron M, Avni A (2010) BAK1 is required for the attenuation of ethylene-inducing xylanase (Eix)-induced defense responses by the decoy receptor LeEix1. *Plant J* 63(5):791–800.
14. Segonzac C, et al. (2011) Hierarchy and roles of pathogen-associated molecular pattern-induced responses in *Nicotiana benthamiana*. *Plant Physiol* 156(2):687–699.
15. Choi SW, et al. (2013) RABA members act in distinct steps of subcellular trafficking of the FLAGELLIN SENSING2 receptor. *Plant Cell* 25(3):1174–1187.
16. Nekrasov V, et al. (2009) Control of the pattern-recognition receptor EFR by an ER protein complex in plant immunity. *EMBO J* 28(21):3428–3438.
17. Chaparro-Garcia A, et al. (2011) The receptor-like kinase SERK3/BAK1 is required for basal resistance against the late blight pathogen *Phytophthora infestans* in *Nicotiana benthamiana*. *PLoS One* 6(1):e16608.
18. Underwood W, Somerville SC (2013) Perception of conserved pathogen elicitors at the plasma membrane leads to relocalization of the Arabidopsis PEN3 transporter. *Proc Natl Acad Sci USA* 110(30):12492–12497.
19. Bauer Z, Gómez-Gómez L, Boller T, Felix G (2001) Sensitivity of different ecotypes and mutants of *Arabidopsis thaliana* toward the bacterial elicitor flagellin correlates with the presence of receptor-binding sites. *J Biol Chem* 276(49):45669–45676.
20. Schwessinger B, et al. (2011) Phosphorylation-dependent differential regulation of plant growth, cell death, and innate immunity by the regulatory receptor-like kinase BAK1. *PLoS Genet* 7(4):e1002046.
21. Sun W, et al. (2012) Probing the Arabidopsis flagellin receptor: FLS2-FLS2 association and the contributions of specific domains to signaling function. *Plant Cell* 24(3):1096–1113.
22. Martins S, et al. (2015) Internalization and vacuolar targeting of the brassinosteroid hormone receptor BRI1 are regulated by ubiquitination. *Nat Commun* 6:6151.
23. Kitakura S, et al. (2011) Clathrin mediates endocytosis and polar distribution of PIN auxin transporters in Arabidopsis. *Plant Cell* 23(5):1920–1931.
24. Li R, et al. (2012) A membrane microdomain-associated protein, Arabidopsis Flot1, is involved in a clathrin-independent endocytic pathway and is required for seedling development. *Plant Cell* 24(5):2105–2122.
25. Bombarely A, et al. (2012) A draft genome sequence of *Nicotiana benthamiana* to enhance molecular plant-microbe biology research. *Mol Plant Microbe Interact* 25(12):1523–1530.
26. Williams RL, Urbé S (2007) The emerging shape of the ESCRT machinery. *Nat Rev Mol Cell Biol* 8(5):355–368.
27. Melotto M, Underwood W, Koczan J, Nomura K, He SY (2006) Plant stomata function in innate immunity against bacterial invasion. *Cell* 126(5):969–980.
28. Smith JM, et al. (2014) Loss of Arabidopsis thaliana dynamin-related protein 2B reveals separation of innate immune signaling pathways. *PLoS Pathog* 10(12):e1004578.

29. Dubiella U, et al. (2013) Calcium-dependent protein kinase/NADPH oxidase activation circuit is required for rapid defense signal propagation. *Proc Natl Acad Sci USA* 110(21):8744–8749.
30. Kadota Y, et al. (2014) Direct regulation of the NADPH oxidase RBOHD by the PRR-associated kinase BIK1 during plant immunity. *Mol Cell* 54(1):43–55.
31. Serrano M, et al. (2007) Chemical interference of pathogen-associated molecular pattern-triggered immune responses in Arabidopsis reveals a potential role for fatty acid synthase type II complex-derived lipid signals. *J Biol Chem* 282(9):6803–6811.
32. Lu D, et al. (2011) Direct ubiquitination of pattern recognition receptor FLS2 attenuates plant innate immunity. *Science* 332(6036):1439–1442.
33. Hao H, et al. (2014) Clathrin and membrane microdomains cooperatively regulate RbohD dynamics and activity in Arabidopsis. *Plant Cell* 26(4):1729–1745.
34. Apostolakos P, Livanos P, Nikolakopoulou TL, Galatis B (2010) Callose implication in stomatal opening and closure in the fern *Asplenium nidus*. *New Phytol* 186(3):623–635.
35. Wu G, et al. (2015) ENHANCED DISEASE RESISTANCE4 associates with CLATHRIN HEAVY CHAIN2 and modulates plant immunity by regulating relocation of EDR1 in Arabidopsis. *Plant Cell* 27(3):857–873.
36. Chaparro-Garcia A, et al. (2015) *Phytophthora infestans* RXLR-WY effector AVR3a associates with dynamin-related protein 2 required for endocytosis of the plant pattern recognition receptor FLS2. *PLoS One* 10(9):e0137071.
37. Bozkurt TO, et al. (2015) Rerouting of plant late endocytic trafficking toward a pathogen interface. *Traffic* 16(2):204–226.
38. Hofius D, et al. (2009) Autophagic components contribute to hypersensitive cell death in Arabidopsis. *Cell* 137(4):773–783.
39. Earley KW, et al. (2006) Gateway-compatible vectors for plant functional genomics and proteomics. *Plant J* 45(4):616–629.
40. Flury P, Klauser D, Schulze B, Boller T, Bartels S (2013) The anticipation of danger: microbe-associated molecular pattern perception enhances AtPep-triggered oxidative burst. *Plant Physiol* 161(4):2023–2035.
41. Grefen C, et al. (2010) A ubiquitin-10 promoter-based vector set for fluorescent protein tagging facilitates temporal stability and native protein distribution in transient and stable expression studies. *Plant J* 64(2):355–365.
42. Geldner N, et al. (2009) Rapid, combinatorial analysis of membrane compartments in intact plants with a multicolor marker set. *Plant J* 59(1):169–178.
43. Dagdas YF, et al. (2016) An effector of the Irish potato famine pathogen antagonizes a host autophagy cargo receptor. *eLife* 5:e10856.
44. Karimi M, Inzé D, Depicker A (2002) GATEWAY vectors for Agrobacterium-mediated plant transformation. *Trends Plant Sci* 7(5):193–195.
45. Mersmann S, Bourdais G, Rietz S, Robatzek S (2010) Ethylene signaling regulates accumulation of the FLS2 receptor and is required for the oxidative burst contributing to plant immunity. *Plant Physiol* 154(1):391–400.
46. Roux M, et al. (2011) The Arabidopsis leucine-rich repeat receptor-like kinases BAK1/ SERK3 and BKK1/SERK4 are required for innate immunity to hemibiotrophic and biotrophic pathogens. *Plant Cell* 23(6):2440–2455.
47. Schneider CA, Rasband WS, Eliceiri KW (2012) NIH Image to ImageJ: 25 years of image analysis. *Nat Methods* 9(7):671–675.